

## From Double-Shelled Grids to Supramolecular Frameworks

Jianfeng Wu, Mei Guo, Xiao-Lei Li, Lang Zhao, Qing-Fu Sun,\* Richard A. Layfield,\* and Jinkui Tang\*

### Experimental Section

General Synthetic Considerations. All chemicals and solvents were commercially obtained and used as received without any further purification. FTIR spectra were measured using a Nicolet 6700 Flex FTIR spectrometer equipped with smart iTR™ attenuated total reflectance (ATR) sampling accessory in the range from 500 to 4000  $\text{cm}^{-1}$ . Elemental analysis for C, H and N were carried out on a Perkin-Elmer 2400 analyzer. Ligand  $\text{H}_4\text{L}'$  (2,6-bis[(6-hydroxymethyl-2-pyridylmethylene)hydrazinecarbonyl]-pyridine) and  $\text{H}_2\text{L}$  (2,6-bis[(2-pyridylmethylene)hydrazinecarbonyl]-pyridine) were synthesized by the similar procedure as reported in the previous literature.<sup>1</sup>

Synthesis of **1·Dy<sub>4</sub>**.  $\text{DyBr}_3 \cdot 6\text{H}_2\text{O}$  (0.1 mmol) was added to a solution of  $\text{H}_4\text{L}'$  (0.1 mmol) in 15 mL methanol/dichloromethane (v:v = 1:2), and then triethylamine (0.2 mmol) was added. After stirred for 5 minutes,  $\text{H}_2\text{L}$  (0.1 mmol) was added into the solution. The resultant yellow solution was stirred for 1 h and subsequently filtered. The filtrate was allowed to slowly evaporate the solvent. Yellow crystals of **1·Dy<sub>4</sub>** suitable for X-ray diffraction analysis were collected after 2 days. Yield in ~55%. Selected IR ( $\text{cm}^{-1}$ ): 3334.37(br), 3164.66(br), 1664.29(m), 1633.44(m), 1587.15(w), 1569.80(w), 1531.23(s), 1569.52(m), 1434.80(m), 1359.59(m), 1303.66(w), 1234.24(m), 1157.10(s), 1114.67(w), 1079.96(m), 1037.53(m), 1016.32(m), 998.96(m), 946.89(w), 842.75(w), 775.25(m), 742.47(w), 647.98(w). Anal. Calcd. for  $[\text{Dy}_4(\text{H}_4\text{L}')_4(\text{H}_2\text{L})_4]\text{Br}_{12} \cdot 28\text{H}_2\text{O}$  ( $\text{C}_{160}\text{H}_{192}\text{Br}_{12}\text{Dy}_4\text{N}_{56}\text{O}_{52}$ , MW = 5340.60): C, 35.98%; H, 3.62%; N, 14.69%. Found: C, 35.81%; H, 3.68%; N, 14.56%.

Synthesis of **2·Dy<sub>4</sub>Cu<sub>4</sub>**.  $\text{DyCl}_3 \cdot 6\text{H}_2\text{O}$  (0.1 mmol) was added to a solution of  $\text{H}_4\text{L}'$  (0.1 mmol) in 15 mL methanol/dichloromethane (v:v = 1:2), and then  $\text{CuCl}_2 \cdot 4\text{H}_2\text{O}$  (0.1 mmol) and triethylamine (0.2 mmol) was added. After stirred for 5 minutes,  $\text{H}_2\text{L}$  (0.1 mmol) was added into the solution. The resultant green solution was stirred for 1 h and subsequently filtered. The filtrate was allowed to slowly evaporate the solvent. Green crystals of **2·Dy<sub>4</sub>Cu<sub>4</sub>** suitable for X-ray diffraction analysis were collected after 3 days. Yield in ~42%. Selected IR ( $\text{cm}^{-1}$ ): 3361.37(br), 1662.37(m), 1641.15(m), 1573.65(s), 1537.01(s), 1434.80(m), 1392.36(m), 1373.09(s), 1290.17(m), 1234.24(m), 1197.10(m), 1159.03(m), 1078.03(m), 1047.17(w), 998.96(w), 941.38(w), 840.83(w), 775.26(w), 744.40(w), 647.98(w). Anal. Calcd. for  $[\text{Dy}_4\text{Cu}_4(\text{H}_2\text{L}')_4(\text{H}_2\text{L})_4\text{Cl}_4(\text{OH})_4]\text{Cl}_4 \cdot 24\text{H}_2\text{O}$  ( $\text{C}_{160}\text{H}_{180}\text{Cl}_8\text{Cu}_4\text{Dy}_4\text{N}_{56}\text{O}_{56}$ , MW = 4971.3): C, 38.65%; H, 3.48%; N, 15.78%. Found: C, 38.69%; H, 3.58%; N, 15.75%.

### Crystallography

Single-crystal X-ray data of the titled complexes were collected on a Bruker Apex II CCD diffractometer equipped with graphite-monochromatized Mo-K $\alpha$  radiation ( $\lambda = 0.71073 \text{ \AA}$ ) at 173(2) K. The structure was solved by direct methods and refined by the full-matrix least-squares method based on  $F^2$  with anisotropic thermal parameters for all non-hydrogen atoms by using the SHELXS (direct methods) and refined by ShelXL (full matrix least squares techniques) in the Olex2 package.<sup>2</sup> Due to the highly disordered solvent molecules in lattice, we use SQUEEZE command to remove the contributions of the highly disorder. The masked electron density of each complex was attached in the crystallography data. All non-hydrogen atoms in the whole structure were refined with anisotropic displacement parameters. Hydrogen atoms were introduced in calculated positions and refined with fixed geometry

with respect to their carrier atoms. Crystallographic data of are listed in Table S1. CCDC 1833798-1833799 contain the supplementary crystallographic data for this paper. These data can be obtained free of charge from the Cambridge Crystallographic Data Centre via [www.ccdc.cam.ac.uk/data\\_request/cif](http://www.ccdc.cam.ac.uk/data_request/cif).

### Magnetic Measurements

Magnetic susceptibility measurements were recorded on a Quantum Design MPMS-XL7 SQUID magnetometer equipped with a 7 T magnet. Direct current (dc) magnetic susceptibility measurements were performed on a polycrystalline sample of **1·Dy<sub>4</sub>** and **2·Dy<sub>4</sub>Cu<sub>4</sub>** in the temperature range 1.9–300 K, in an applied field of 1000 Oe. The dynamics of the magnetization were investigated from the ac susceptibility measurements in the zero static fields and a 3.0 Oe ac oscillating field. Diamagnetic corrections were made with the Pascal's constants<sup>3</sup> for all the constituent atoms as well as the contributions of the sample holder.

Table S1. Crystallographic data for complexes **1·Dy<sub>4</sub>** and **2·Dy<sub>4</sub>Cu<sub>4</sub>**.

	<b>1·Dy<sub>4</sub></b>	<b>2·Dy<sub>4</sub>Cu<sub>4</sub></b>
Formula	C <sub>160</sub> H <sub>192</sub> Br <sub>12</sub> Dy <sub>4</sub> N <sub>56</sub> O <sub>52</sub>	C <sub>160</sub> H <sub>180</sub> Cl <sub>8</sub> Cu <sub>4</sub> Dy <sub>4</sub> N <sub>56</sub> O <sub>56</sub>
FW, g·mol <sup>-1</sup>	5340.60	4971.3
crystal system	Cubic	Cubic
space group	<i>Ia-3d</i>	<i>Ia-3d</i>
<i>T</i> , K	173.0	173.0
$\lambda$ , Å	0.71073	0.71073
<i>a</i> , Å	63.740(5)	63.821(2)
<i>b</i> , Å	63.740(5)	63.821(2)
<i>c</i> , Å	63.740(5)	63.821(2)
$\alpha$ , °	90	90
$\beta$ , °	90	90
$\gamma$ , °	90	90
<i>V</i> , Å <sup>3</sup>	258961(55)	259954(26)
<i>Z</i>	24	24
reflns collected	54355	229429
unique reflns	6469	19084
R <sub>int</sub>	0.0604	0.1049
GOF on <i>F</i> <sup>2</sup>	1.053	1.071
<i>R</i> <sub>1</sub> <sup>a</sup> , <i>wR</i> <sub>2</sub> ( <i>I</i> ≥ 2 $\sigma$ ( <i>I</i> )) <sup>b</sup>	0.1005, 0.2455	0.1062, 0.2563
<i>R</i> <sub>1</sub> , <i>wR</i> <sub>2</sub> ( <i>all data</i> )	0.1469, 0.2946	0.1675, 0.3106
CCDC number	1833798	1833799

$$^a) R_1 = \frac{\sum ||F_o| - |F_c||}{\sum |F_o|}, \quad ^b) wR_2 = \left[ \frac{\sum w(F_o^2 - F_c^2)^2}{\sum w(F_o^2)^2} \right]^{1/2}$$

Table S2. Selected bond distances (Å) for complexes **1·Dy<sub>4</sub>** and **2·Dy<sub>4</sub>Cu<sub>4</sub>**.

	<b>1·Dy<sub>4</sub></b>		<b>2·Dy<sub>4</sub>Cu<sub>4</sub></b>
Dy(1)-O(1)	2.407(14)	Dy(1)-O(1)	2.399(6)
Dy(1)-N(3)	2.427(19)	Dy(1)-N(3)	2.460(11)
Dy(1)-N(10)	2.486(18)	Dy(1)-N(10)	2.478(9)
Dy(1)-O(13)	2.421(13)	Dy(1)-O(13)	2.392(7)
Dy(1)-O(21)	2.403(14)	Dy(1)-O(21)	2.356(7)
Dy(1)-N(23)	2.494(19)	Dy(1)-N(23)	2.489(8)
Dy(1)-N(25)	2.549(18)	Dy(1)-N(25)	2.493(10)
Dy(1)-O(32)	2.417(16)	Dy(1)-O(32)	2.427(8)
Dy(1)-O(10)	2.430(14)	Dy(1)-O(11)	2.450(7)

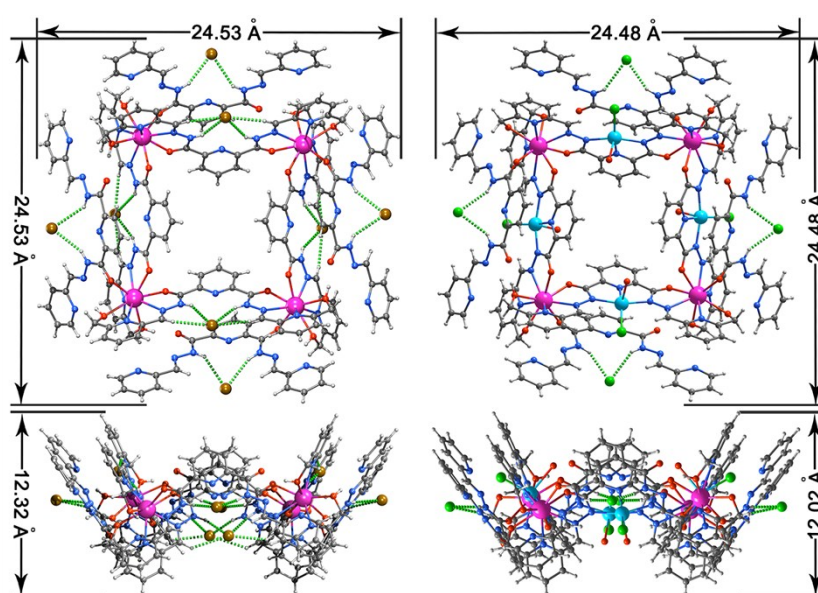


Fig. S1 Views of complexes **1·Dy<sub>4</sub>** (left) and **2·Dy<sub>4</sub>Cu<sub>4</sub>** (right) along *c* axis (top) and *b* axis (bottom) with parameter labels. The pink, azure, brown, green, blue, dark, red and grey spheres represent Dy, Cu, Br, Cl, N, C, O and H, respectively. Solvents have been omitted for clarity.

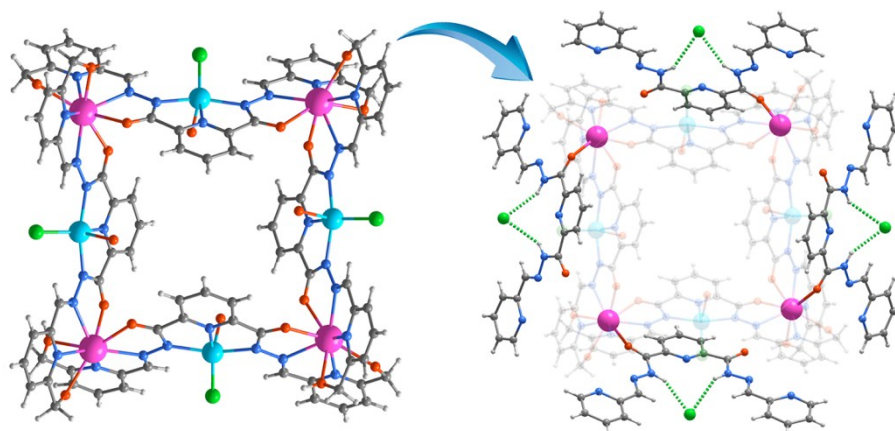


Fig. S2 Inner grid (left) and outer shell (right) of **2·Dy<sub>4</sub>Cu<sub>4</sub>**. Solvents have been omitted for clarity.

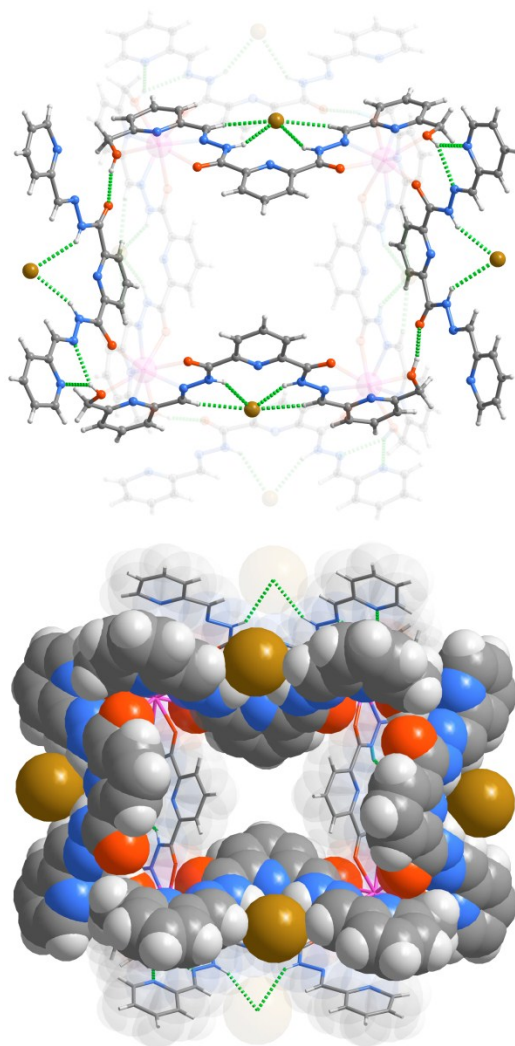


Fig. S3 Intramolecular hydrogen bonding between ligands  $H_4L'$  and  $H_2L$  (top) and the relevant space filling mode (bottom) of  $1 \cdot Dy_4$ . The pink, brown, blue, dark, red and grey spheres represent Dy, Br, N, C, O and H, respectively. Solvents have been omitted for clarity.

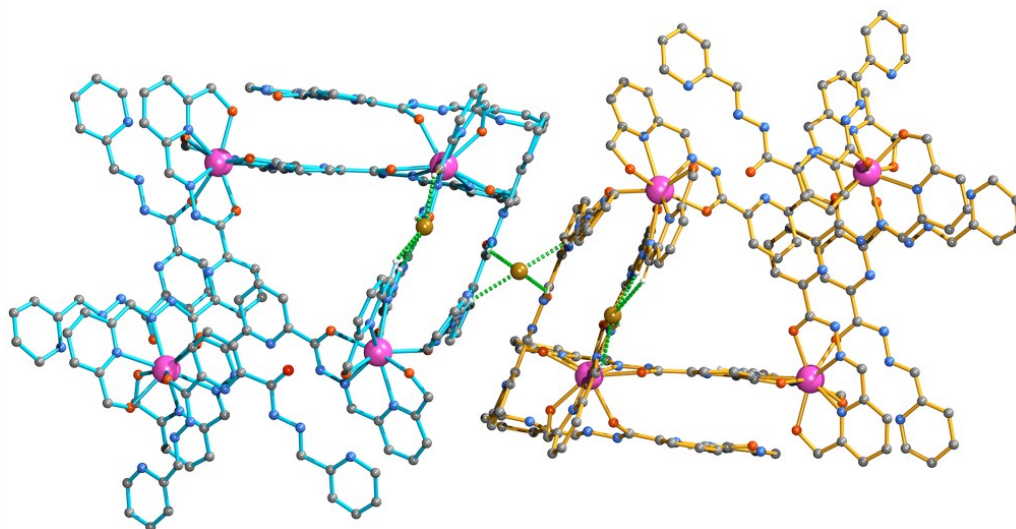


Fig. S4 Stacking and hydrogen bonding mode of the nearest molecules of  $1 \cdot Dy_4$  through hydrogen bonding.

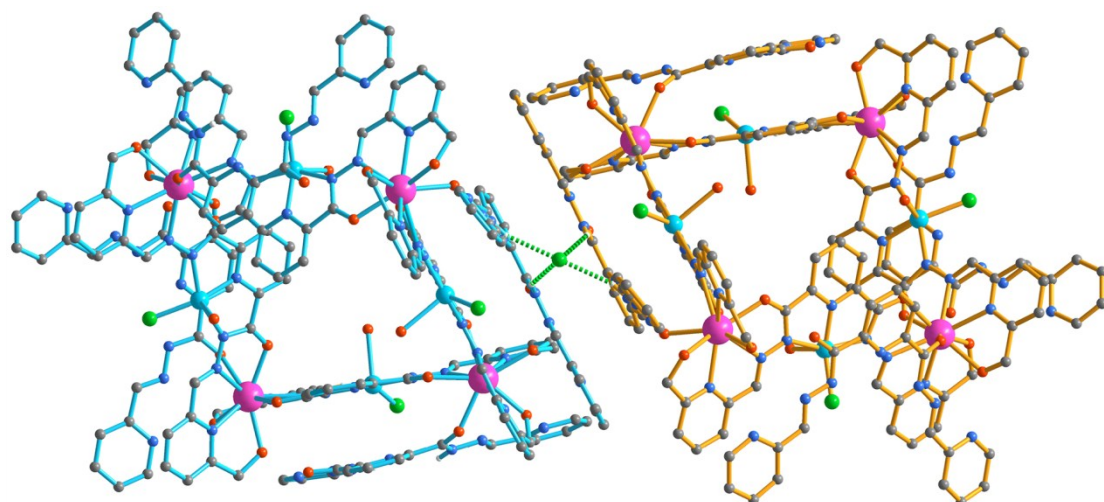


Fig. S5 Stacking and hydrogen bonding mode of the nearest molecules of  $2 \cdot \text{Dy}_4\text{Cu}$  through hydrogen bonding.

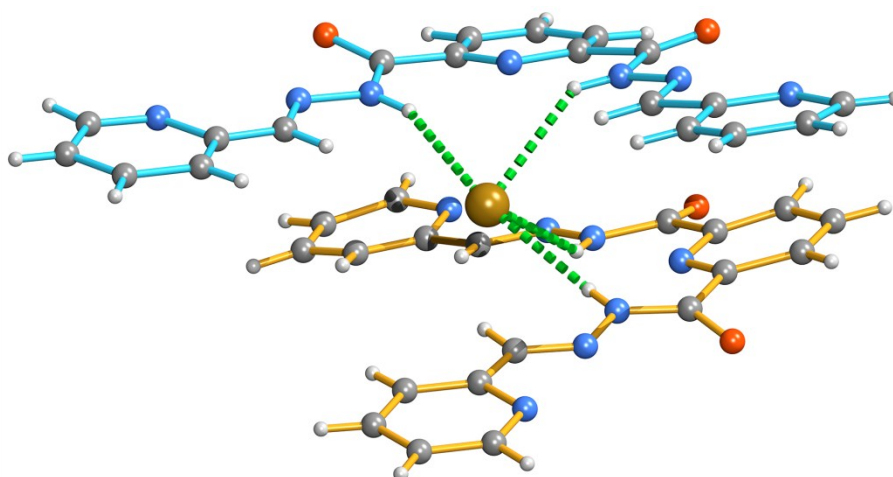


Fig. S6 Ligands stacking and hydrogen bonding mode of two neighboring  $\text{H}_2\text{L}$  ligands in  $1 \cdot \text{Dy}_4$ .

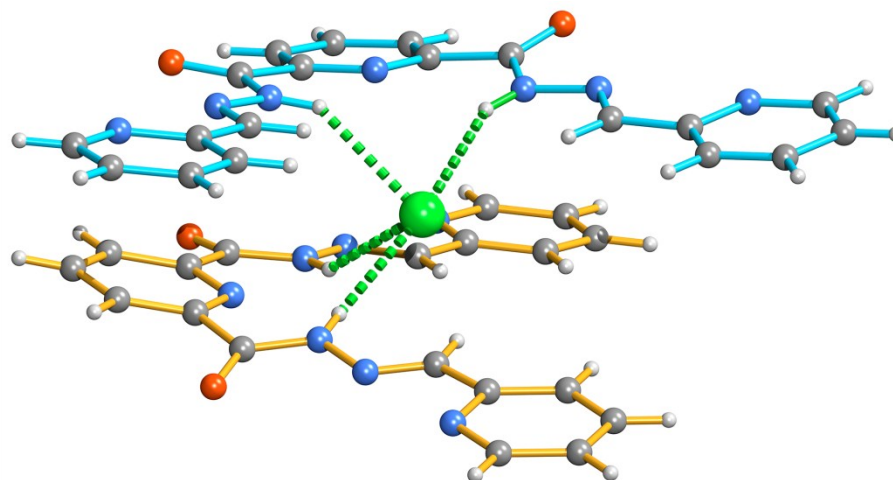


Fig. S7 Ligands stacking and hydrogen bonding mode of two neighboring  $\text{H}_2\text{L}$  ligands in  $2 \cdot \text{Dy}_4\text{Cu}$ .

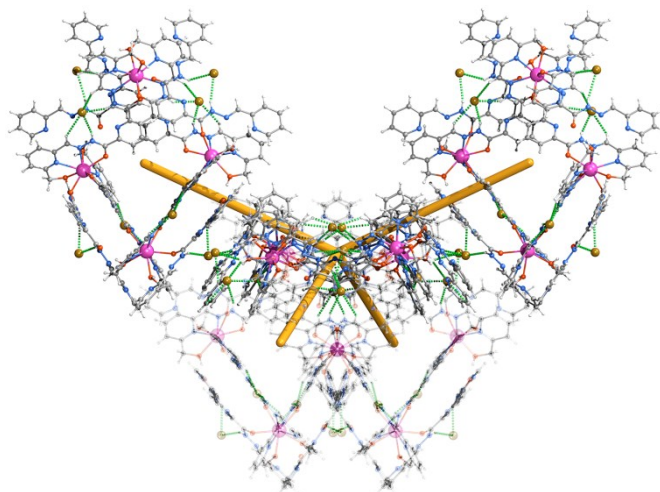


Fig. S8 Molecular packing modes of the nearest molecules of  $1 \cdot \text{Dy}_4$ . The orange sticks represent the connection of the nearest two molecules through ligands stacking and hydrogen bonding.

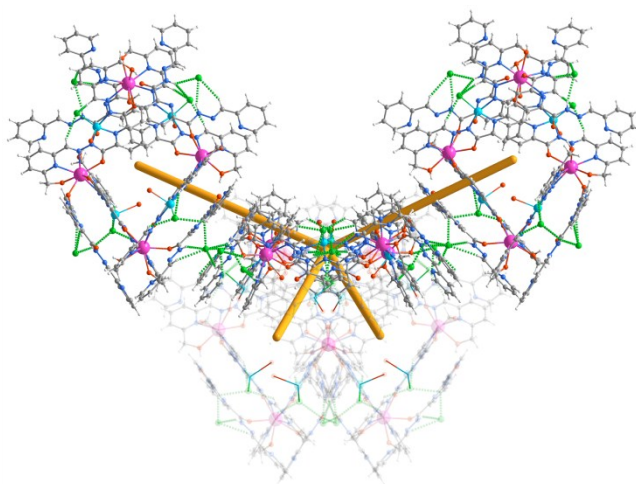


Fig. S9 Molecular packing models of the nearest molecules of  $2 \cdot \text{Dy}_4\text{Cu}_4$ . The orange sticks represent the connection of the nearest two molecules through ligands stacking and hydrogen bonding.

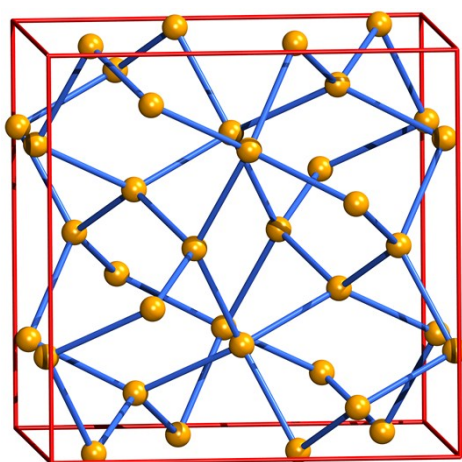


Fig. S10 Molecular distribution in the unit cell of both complexes  $1 \cdot \text{Dy}_4$  and  $2 \cdot \text{Dy}_4\text{Cu}_4$  with orange sphere representing the molecules.

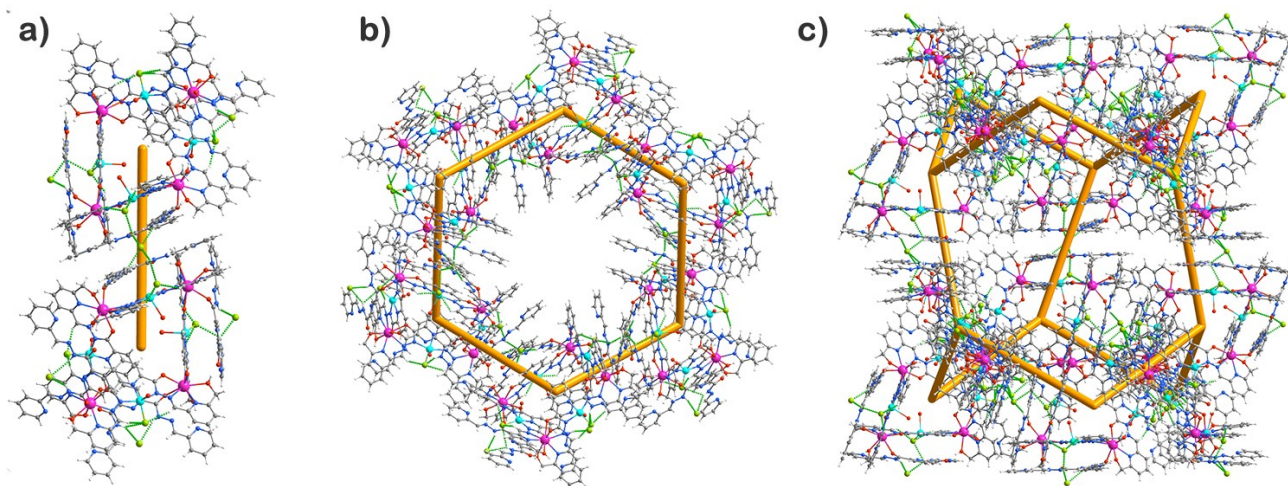


Fig. S11 Molecular packing modes of  $2 \cdot \text{Dy}_4\text{Cu}_4$ . a) the stick-like linker mode of nearest two molecules through hydrogen bonding; b) double-shelled grids assembled into macrocycle; c) the final Lonsdaleite topology.

Table S3. The *CSHM* values calculated by *SHAPE* 2.1 for  $1 \cdot \text{Dy}_4$  and  $2 \cdot \text{Dy}_4\text{Cu}_4$ .

Coordination Geometry	$1 \cdot \text{Dy}_4$	$2 \cdot \text{Dy}_4\text{Cu}_4$
Johnson triangular cupola J3 ( $C_{3v}$ )	14.069	14.908
Capped cube J8 ( $C_{4v}$ )	10.657	10.514
Spherical-relaxed capped cube ( $C_{4v}$ )	9.094	8.888
Capped square antiprism J10 ( $C_{4v}$ )	2.777	2.184
Spherical capped square antiprism ( $C_{4v}$ )	1.884	1.402
Tricapped trigonal prism J51 ( $D_{3h}$ )	4.363	4.028
Spherical tricapped trigonal prism ( $D_{3h}$ )	1.976	1.810

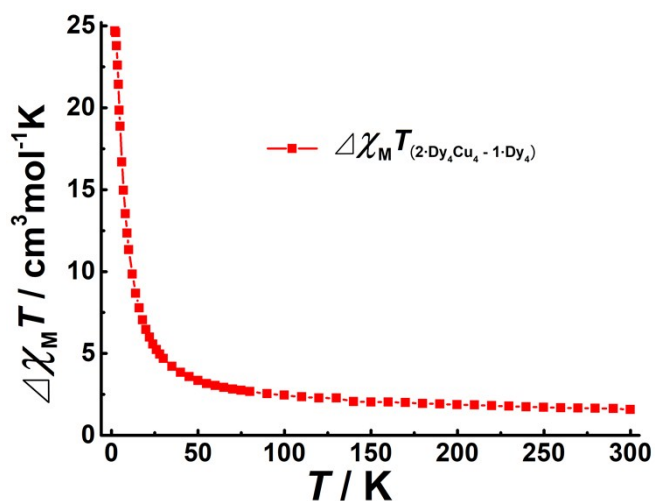


Fig. S12 Extracted temperature dependence of  $\Delta\chi_{\text{M}}T$  products from  $[2 \cdot \text{Dy}_4\text{Cu}_4] - [1 \cdot \text{Dy}_4]$  at 1 kOe between 2 and 300 K.

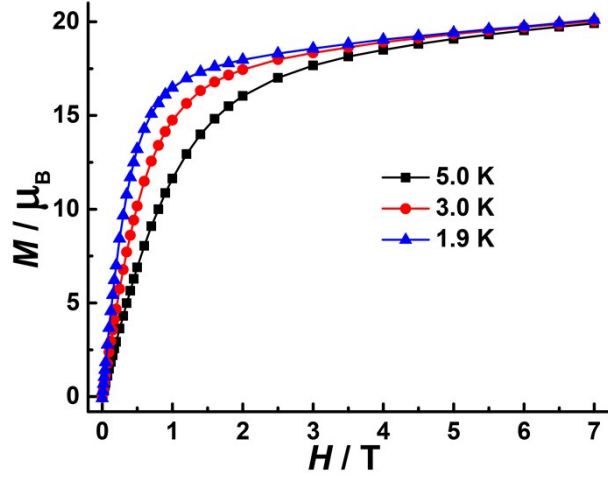


Fig. S13 Molar magnetization ( $M$ ) vs. magnetic field ( $H$ ) for  $1 \cdot \text{Dy}_4$  at 1.9, 3.0 and 5.0 K.

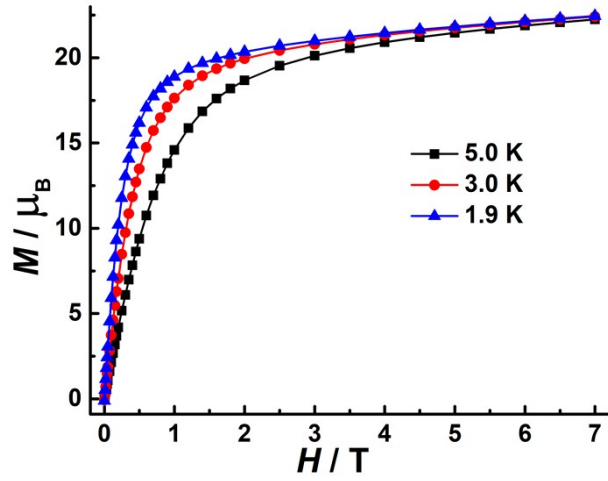


Fig. S14 Molar magnetization ( $M$ ) vs. magnetic field ( $H$ ) for  $2 \cdot \text{Dy}_4\text{Cu}_4$  at 1.9, 3.0 and 5.0 K.

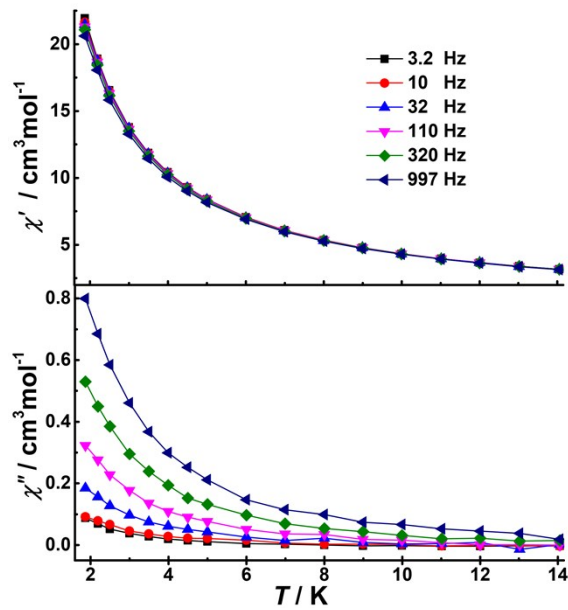


Fig. S15 Temperature dependence of ac susceptibility for  $1 \cdot \text{Dy}_4$  at indicated frequencies under zero dc field.

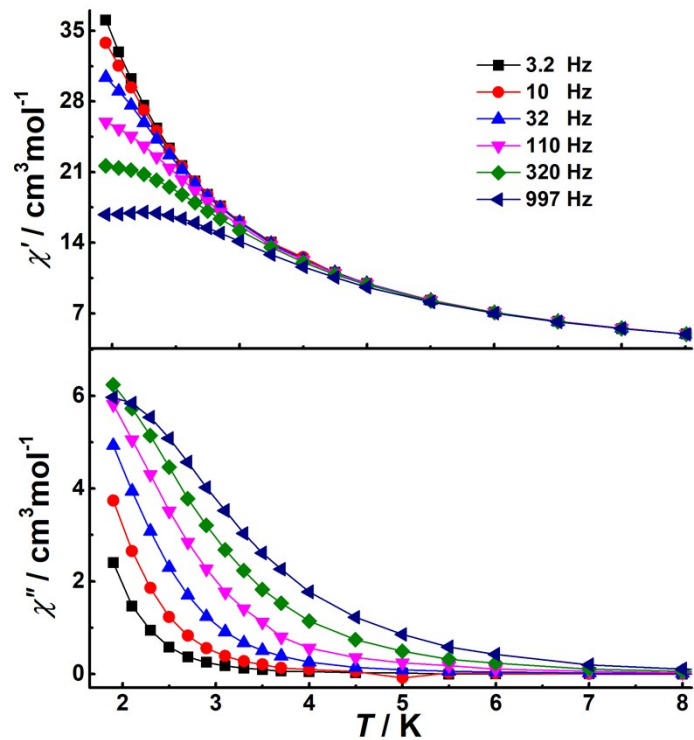


Fig. S16 Temperature dependence of ac susceptibility for  $2 \cdot \text{Dy}_4\text{Cu}_4$  at indicated frequencies under zero dc field.

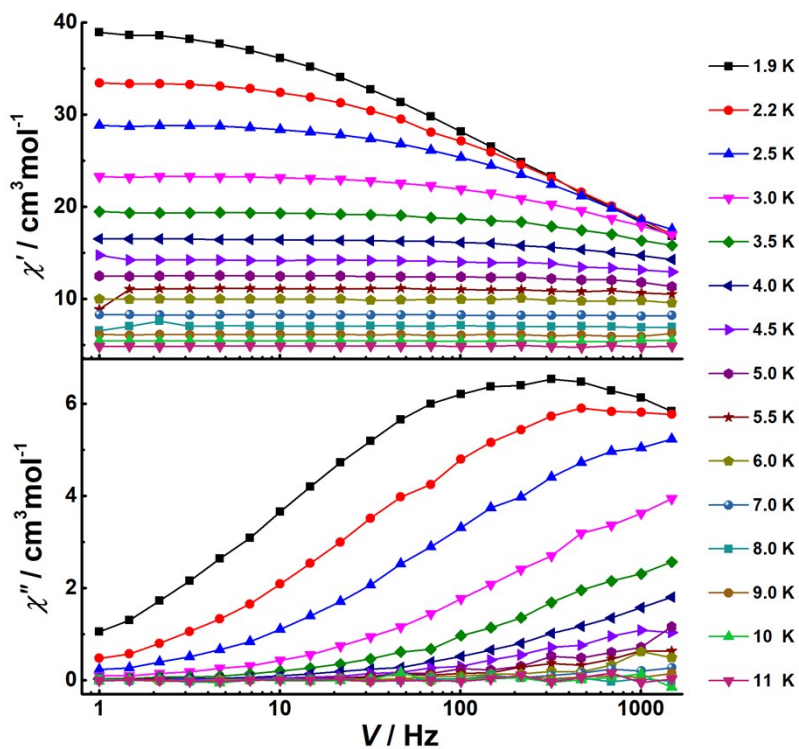


Fig. S17 Frequency dependence of ac susceptibility for  $2 \cdot \text{Dy}_4\text{Cu}_4$  at indicated temperature under zero dc field.

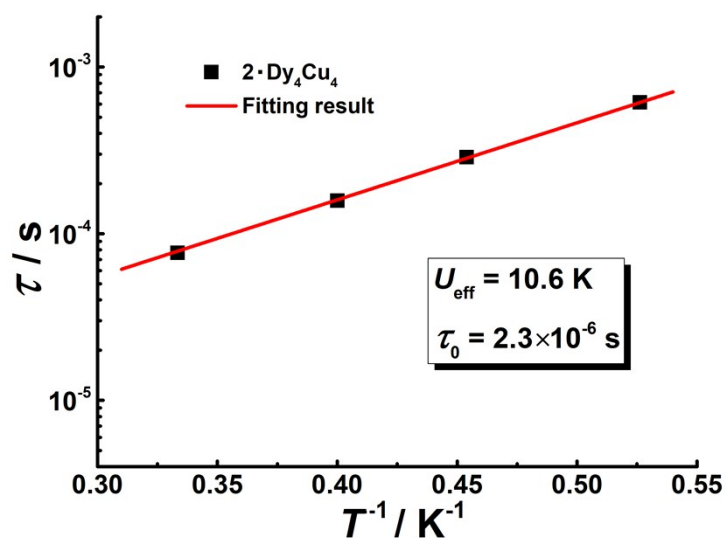


Fig. S18 Plot of  $\tau$  vs.  $T^{-1}$  for  $2 \cdot \text{Dy}_4\text{Cu}_4$  obtained under zero dc fields over the temperature range 1.9–3.0 K. The red line represents the Arrhenius fitted result.

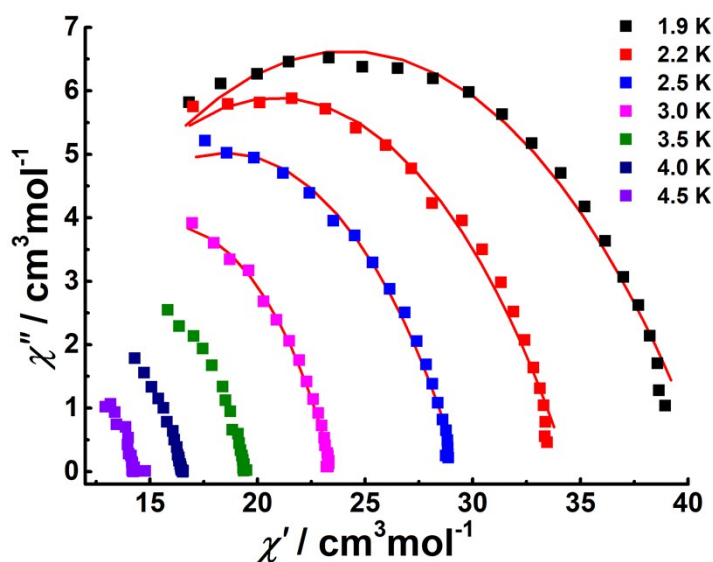


Fig. S19 Cole-Cole plots for  $2 \cdot \text{Dy}_4\text{Cu}_4$  at zero field between 1.9 and 4.5 K. The solid lines indicate the best fits to the experiments with the generalized Debye model.

## Reference

- (a) M. U. Anwar, S. S. Tandon, L. N. Dawe, F. Habib, M. Murugesu and L. K. Thompson, *Inorg. Chem.*, 2011, **51**, 1028-1034; (b) L. N. Dawe and L. K. Thompson, *Angew. Chem. Int. Ed.*, 2007, **46**, 7440-7444; (c) L. Zhao, C. J. Matthews, L. K. Thompson and S. L. Heath, *Chem. Commun.*, 2000, **0**, 265-266; (d) A. Adhikary, H. S. Jena, S. Khatua and S. Konar, *Chem. Asian J.*, 2014, **9**, 1083-1090.
- (a) G. M. Sheldrick, *SHELXS-97 Program for Crystal Structure Solution*, University of Göttingen: Germany, 1997; (b) *Acta Crystallogr., Sect. A*, 2008, **64**, 112-122.
- E. A. Boudreaux and L. N. Mulay, *Theory and Applications of Molecular Paramagnetism*, John Wiley & Sons, New York, 1976.